ISSN 1070-3284, Russian Journal of Coordination Chemistry, 2017, Vol. 43, No. 6, pp. 396–403. © Pleiades Publishing, Ltd., 2017.

Synthesis, Characterization, Crystal Structures, and Antibacterial Activity of Oxidovanadium(V) Complexes with Mixed Ligands[1]

X. Y. Qiu[a], *, S. J. Liu[a], J. X. Lei[b], **, and Y. T. Ye[a]

[a]*College of Science & Technology, Ningbo University, Ningbo, 315212 P.R. China*

[b]*College of Chemistry and Chemical Engineering, Jinzhong University, Jinzhong, 030619 P.R. China*

**e-mail: xiaoyang_qiu@126.com*

*** e-mail: leijinxianjz@sohu.com*

Received May 5, 2016

Abstract—Two new oxidovanadium(V) complexes, [VO(L)(Ehp)] (**I**) and [VO(L)(Aha)] (**II**), where L is the dianionic form of 4-bromo-*N*'-(4-oxopentan-2-ylidene)benzohydrazide (H_2L), Ehp is the monoanionic form of 2-ethyl-3-hydroxy-4*H*-pyran-4-one (HEhp), and Aha is the monoanionic form of acetohydroxamic acid (HAha), were prepared and characterized by elemental analysis, infrared and electronic spectra, and ^{1}H NMR spectra. Structures of the complexes were further confirmed by single crystal X-ray diffraction (CIF files CCDC nos. 1477847 (**I**), 1477850 (**II**)). H_2L coordinates to the V atom through the two enolic O atoms and the imino N atom. The ligands Ehp and Aha coordinate to the V atoms through bidentate OO donor set. The V atoms of the complexes are in octahedral coordination, with the oxo group furnished the octahedral geometry. The complexes show effective antibacterial activity against *Bacillus subtilis*.

Keywords: Schiff base, oxidovanadium complex, mixed ligands, crystal structure, antibacterial activity

DOI: 10.1134/S1070328417060069

INTRODUCTION

Among various metal complexes, those derived from Schiff bases have received much attention in biological and medicinal chemistry [1–4]. Vanadium complexes have been reported to have interesting biological activities such as normalizing the high blood glucose levels and acting as models of haloperoxidases [5–7]. In addition, vanadium complexes have shown effective antibacterial activities [8–10]. Recently, our research group has reported a few vanadium complexes with biological properties [11–13]. In order to explore new vanadium-based materials, in the present paper, two new oxidovanadium(V) complexes, [VO(L)(Ehp)] (**I**) and [VO(L)(Aha)] (**II**), where L is the dianionic form of 4-bromo-*N*'-(4-oxopentan-2-ylidene)benzohydrazide (H_2L), Ehp is the monoanionic form of 2-ethyl-3-hydroxy-4*H*-pyran-4-one (HEhp), and Aha is the monoanionic form of acetohydroxamic acid (HAha), were prepared, characterized and studied on their antibacterial activity.

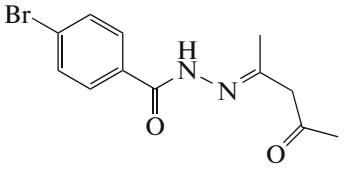

H_2L

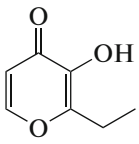

HEhp

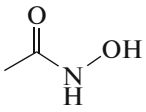

HAha

EXPERIMENTAL

Materials and measurements. Commercially available 4-bromobenzohydrazide were purchased from Aldrich and used without further purification. Other solvents and reagents were made in China and used as received. C, H, and N elemental analyses were performed with a Perkin-Elmer 240 elemental analyzer. Infrared spectra were recorded on a Nicolet

[1] The article is published in the original.

AVATAR 360 spectrometer as KBr pellets in the 4000–400 cm^{-1} region. UV-Vis spectra were recorded on a Lambda 900 spectrometer. ^1H NMR spectra were recorded on a Bruker 300 MHz spectrometer. Thermogravimetric (TG) analysis was performed on a Perkin-Elmer Pyris Diamond TG-DTA thermal analyses system.

Synthesis of complex I. 4-Bromobenzohydrazide (0.1 mmol, 29.7 mg), HEhp (0.1 mmol, 14.0 mg), and $VO(Acac)_2$ (0.1 mmol, 26.5 mg) were dissolved in methanol (15 mL). The mixture was stirred at room temperature for 30 min to give a brown solution. After keeping the solution in air for a few days, brown block-shaped single crystals suitable for X-ray crystal structure determination were obtained. The crystals were isolated by filtration and dried in a vacuum desiccator containing anhydrous $CaCl_2$. The yield was 41%.

IR data (KBr; ν_{max}, cm^{-1}): 3120, 3072, 2926, 2856, 1598, 1538, 1483, 1442, 1390, 1335, 1260, 1187, 1131, 1097, 1016, 1020, 980, 949, 835, 785, 721, 638, 591, 533, 468, 437. UV-Vis data in acetonitrile (λ, nm (ε, L mol^{-1} cm^{-1})): 273 (17150), 331 (6560). ^1H NMR (300 MHz; DMSO-d^6; δ, ppm): 8.48 (d., 1H, Ar*H*), 7.72–7.62 (m., 4H, Ar*H*), 6.70 (d., 1H, Ar*H*), 5.63 (s., 1H, C*H*), 3.35 (s., 3H, CH_3), 3.02 (q., 2H, CH_2CH_3), 2.17 (s., 3H, CH_3), 1.35 (t., 3H, CH_2CH_3).

For $C_{19}H_{18}N_2O_6BrV$

anal. calcd., %:	C, 45.53;	H, 3.62;	N, 5.59.
Found, %:	C, 45.38;	H, 3.73;	N, 5.46.

Synthesis of complex II. 4-Bromobenzohydrazide (0.1 mmol, 29.7 mg), HAha (0.1 mmol, 7.5 mg) and $VO(Acac)_2$ (0.1 mmol, 26.5 mg) were dissolved in methanol (15 mL). The mixture was stirred at room temperature for 30 min to give a brown solution. After keeping the solution in air for a few days, brown block-shaped single crystals, suitable for X-ray crystal structure determination, were obtained. The crystals were isolated by filtration and dried in a vacuum desiccator containing anhydrous $CaCl_2$. The yield was 55%.

IR data (KBr; ν_{max}, cm^{-1}): 3321, 3057, 3002, 2960, 2926, 1597, 1545, 1492, 1390, 1328, 1285, 1125, 1010, 962, 838, 798, 727, 681, 622, 579, 567, 486. UV-Vis data in acetonitrile (λ, nm (ε, L mol^{-1} cm^{-1})): 275 (18535), 345 (9400), 454 (6,365). ^1H NMR (300 MHz, DMSO-d^6; δ, ppm): 13.86 (s., 1H, N*H*), 7.77 (d., 2H, Ar*H*), 7.66 (d., 2H, Ar*H*), 5.54 (s., 1H, C*H*), 3.32 (s., 3H, CH_3), 2.19 (s., 3H, CH_3), 2.12 (s., 3H, CH_3).

For $C_{14}H_{15}N_3O_5BrV$

anal. calcd., %:	C, 38.55;	H, 3.47;	N, 9.63.
Found, %:	C, 38.72;	H, 3.54;	N, 9.49.

X-ray crystallography. Diffraction intensities for the complexes were collected at 298(2) K using a Bruker D8 VENTURE PHOTON diffractometer with MoK_α radiation (λ = 0.71073 Å). The collected data were reduced using SAINT [14], and multi-scan absorption corrections were performed using SADABS [15]. Structures of the complexes were solved by direct methods and refined against F^2 by full-matrix least-squares methods using SHELXTL [16]. All of the non-hydrogen atoms were refined anisotropically. The amino hydrogen atom in complex **II** was located from a difference Fourier map and refined isotropically. The remaining hydrogen atoms were placed in idealized positions and constrained to ride on their parent atoms. Crystallographic data for the complexes are summarized in Table 1. Selected bond lengths and angles are given in Table 2.

Crystallographic data for structures **I** and **II** has been deposited with the Cambridge Crystallographic Data Centre (CCDC nos. 1477847 (**I**), 1477850 (**II**); deposit@ccdc.cam.ac.uk or www: http://www.ccdc.cam.ac.uk).

Antibacterial assay. The antibacterial activity of the complexes was tested against *B. subtilis*, *S. aureus*, *E. coli*, and *P. aeruginosa* using LB medium (Luria–Bertani medium: tryptone 10 g, yeast extract 5 g, NaCl 10 g, distilled water 1000 mL, pH 7.4). The IC_{50} (half inhibitory concentration) of the test compounds were determined by a colorimetric method using the dye MTT (3-(4,5-di-methylth-iazol-2-yl)-2,5-diphenyl tetrazolium bromide).

A stock solution of the synthesized compound (1000 μg mL^{-1}) in DMSO was prepared and graded quantities of the test compounds were incorporated in specified quantity of sterilized liquid LB medium. Suspension of the microorganism was prepared and applied to 96-well assay plate with serially diluted compounds to be tested. 10 μL of tested samples at pre-set concentrations were added to wells with penicillin as a positive reference, and with the solvent control (5% DMSO) in medium and incubated at 37°C for 24 h.

After 24 h exposure, 10 μL of PBS (phosphate buffered saline 0.01 mol L^{-1}, pH 7.4) containing 4 mg mL^{-1} of MTT was added to each well. After 4 h, the medium was replaced by 150 μL DMSO to dissolve the complexes. The absorbance at 492 nm of each well was measured with an ELISA plate reader. The IC_{50} value was defined as the concentration at which 50% of the bacterial strain could survive.

RESULTS AND DISCUSSION

The complexes were prepared by the reaction of 4-bromobenzohydrazide with $VO(Acac)_2$ and HEhp or HAha in methanol. The ligand L was formed by the condensation reaction of 4-bromobenzohydrazide

Table 1. Crystallographic data and refinement parameters for complexes **I** and **II**

Parameter	Value	
	I	**II**
Mr	501.20	436.14
Crystal color, habit	Brown, block	Brown, block
Crystal size, mm^3	0.28 × 0.26 × 0.22	0.23 × 0.23 × 0.18
Crystal system	Monoclinic	Orthorhombic
Space group	$P2_1/n$	*Pbca*
a, Å	12.054(1)	17.639(3)
b, Å	7.657(2)	8.252(1)
c, Å	22.582(2)	23.627(4)
β, deg	90.629(2)	
V, $Å^3$	2084.2(6)	3439.2(10)
Z	4	8
ρ_{calcd}, g cm^{-3}	1.597	1.685
μ, mm^{-1}	2.431	2.929
F(000)	1008	1744
Number of unique data	3009	3040
Number of observed data ($I > 2\sigma(I)$)	1567	2011
Number of parameters	264	223
Number of restraints	0	1
R_1, wR_2 ($I > 2\sigma(I)$)	0.0794, 0.1948	0.0469, 0.0794
R_1, wR_2 (all data)	0.1617, 0.2275	0.0919, 0.0916
Goodness of fit on F^2	1.029	1.082
Largest peak and deepest hole, *e* $Å^{-3}$	0.413, –0.345	0.388, –0.222

with acetylacetone. Crystals of the complexes are soluble in DMF, DMSO, methanol, ethanol, and acetonitrile.

Molecular structure of complex **I** is shown in Fig. 1a. The V atom in the complex is in octahedral coordination, with the two enalate O atoms and the imino N atom of L, and the phenolate O atom of Ehp ligand defining the equatorial plane, and with the carbonyl O atom of Ehp ligand and the oxo group locating at the axial positions. The V atom deviates from the least-squares plane defined by the equatorial atoms by 0.313(1) Å. The coordinate bond lengths in the complex are similar to those observed in vanadium complexes with hydrazone ligands [17, 18]. The distortion of the octahedral coordination can be observed from the coordinate bond angles, ranging from 75.8(2)° to 102.1(2)° for the perpendicular angles, and from 154.1(2)° to 176.3(3)° for the diagonal angles. The dihedral angle between the C(1)–C(6) and C(13)–C(17)/O(5) planes is 99.0(3)°. In the crystal structure of the complex, molecules are stacked via weak π···π interactions along the *y* axis (Fig. 2a).

Molecular structure of complex **II** is shown in Fig. 1b. The V atom in the complex is in octahedral

Table 2. Selected bond distances (Å) and angles (deg) for complexes **I** and **II**

Bond	*d*, Å	Bond	*d*, Å
		I	
V(1)–O(1)	1.934(6)	V(1)–O(2)	1.883(6)
V(1)–O(3)	1.875(5)	V(1)–O(4)	2.272(4)
V(1)–O(6)	1.571(6)	V(1)–N(2)	2.055(6)
		II	
V(1)–O(1)	1.946(2)	V(1)–O(2)	1.877(2)
V(1)–O(3)	2.191(3)	V(1)–O(4)	1.870(3)
V(1)–O(5)	1.589(3)	V(1)–N(2)	2.031(3)
Angle	ω, deg	Angle	ω, deg
		I	
O(6)V(1)O(3)	99.6(2)	O(6)V(1)O(2)	98.0(3)
O(3)V(1)O(2)	102.1(2)	O(6)V(1)O(1)	100.7(4)
O(3)V(1)O(1)	92.3(2)	O(2)V(1)O(1)	154.1(2)
O(6)V(1)N(2)	99.2(3)	O(3)V(1)N(2)	159.3(2)
O(2)V(1)N(2)	83.7(2)	O(1)V(1)N(2)	75.8(2)
O(6)V(1)O(4)	176.3(3)	O(3)V(1)O(4)	76.86(18)
O(2)V(1)O(4)	81.7(2)	O(1)V(1)O(4)	80.7(2)
N(2)V(1)O(4)	84.40(19)		
		II	
O(5)V(1)O(4)	94.79(14)	O(5)V(1)O(2)	98.49(13)
O(4)V(1)O(2)	107.58(11)	O(5)V(1)O(1)	100.61(13)
O(4)V(1)O(1)	87.46(11)	O(2)V(1)O(1)	154.54(11)
O(5)V(1)N(2)	99.94(13)	O(4)V(1)N(2)	159.48(12)
O(2)V(1)N(2)	84.38(11)	O(1)V(1)N(2)	75.89(11)
O(5)V(1)O(3)	170.41(13)	O(4)V(1)O(3)	76.10(11)
O(2)V(1)O(3)	81.72(10)	O(1)V(1)O(3)	82.21(10)
N(2)V(1)O(3)	89.63(11)		

coordination, with the two enalate O atoms and the imino N atom of L, and the deprotonated hydroxyl O atom of Aha ligand defining the equatorial plane, and with the carbonyl O atom of Aha ligand and the oxo group locating at the axial positions. The V atom deviates from the least-squares plane defined by the equatorial atoms by 0.273(1) Å. The coordinate bond lengths in the complex are comparable to those of complex **I**, and also similar to those observed in vanadium complexes with hydrazone ligands [17, 18]. The distortion of the octahedral coordination can be observed from the coordinate bond angles, ranging from 75.89(11)° to 107.58(11)° for the perpendicular angles, and from 154.54(11)° to 170.41(13)° for the diagonal angles. The dihedral angle between the C(1)–C(6) and O(3)/C(14)/N(3)/O(4) planes is 69.8(4)°. In the crystal structure of the complex, molecules are linked through intermolecular N–H···O hydrogen bonds (N(3)–H(3*A*) 0.90(1), H(3*A*)···O(5)^{i} 2.26(3), N(3)···O(5)^{i} 3.046(5) Å, N(3)–H(3*A*)···O(5)^{i}

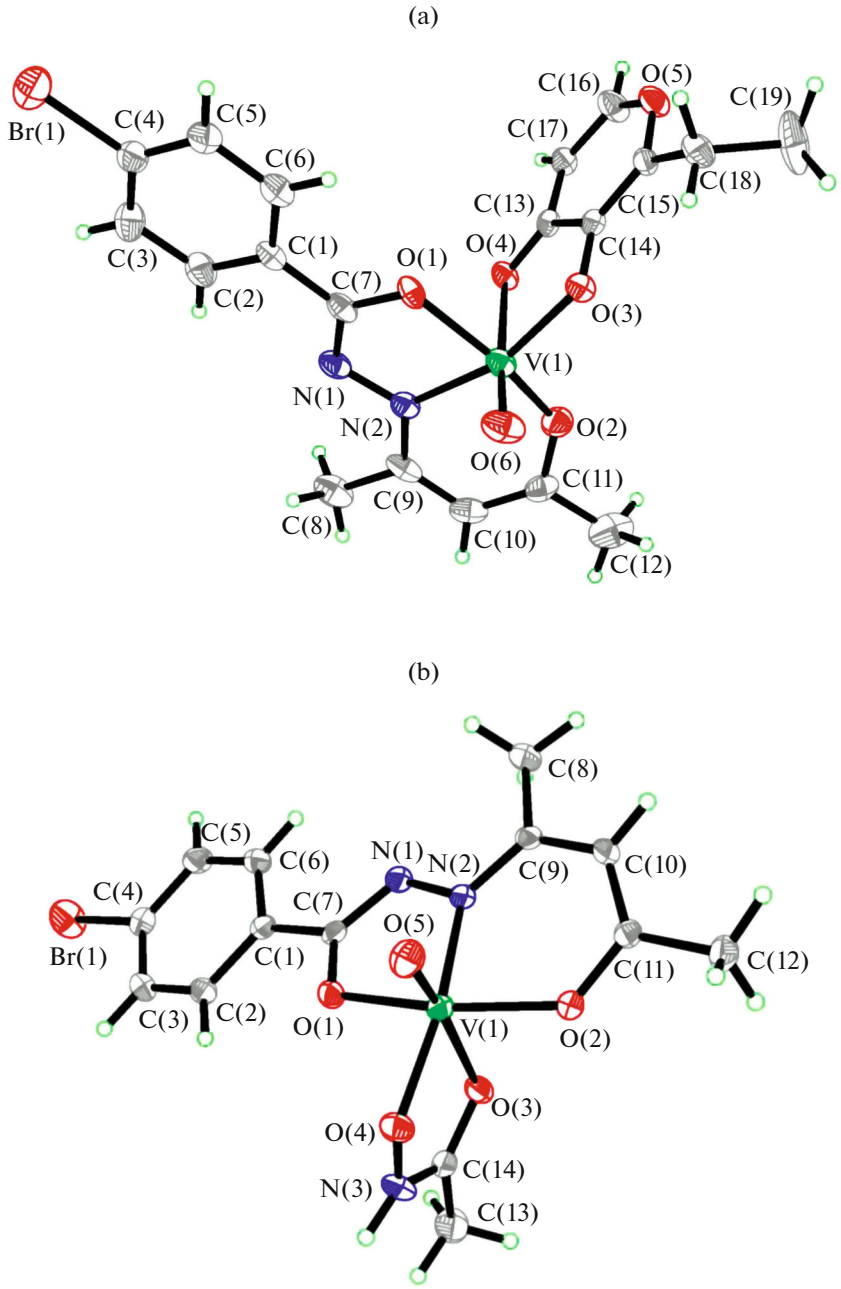

Fig. 1. Molecular structures of **I** (a) and **II** (b) showing the atom-numbering scheme. Displacement ellipsoids are drawn at the 30% probability level.

147(4)°; N(3)–H(3*A*) 0.90(1), H(3*A*)···O(1)^{i} 2.47(3), N(3)···O(1)^{i} 3.228(4) Å, N(3)–H(3*A*)···O(1)^{i} 142(4)°; ^{i} 3/2 – *x*, 1/2 + *y*, *z*) to form chains along the *y* axis (Fig. 2b).

The sharp and medium band at 3321 cm^{-1} for the spectrum of **II** is due to the vibration of the N–H group. The ν(C=N) absorptions are observed at 1598 cm^{-1} for **I** and 1597 cm^{-1} for **II** [19]. The intense bands indicative of the C=O vibrations are absent in the complexes, indicating the enolization of the ligands. The weak peaks in the low wave numbers in the region 400–650 cm^{-1} may be attributed to V–O and V–N bonds in the complexes. Complexes **I** and **II** exhibit typical bands at 980 and 962 cm^{-1}, respectively, which are assigned to the V=O vibrations [20].

The UV-Vis spectra of complexes **I**, **II** (Fig. 3) were recorded in 10^{-5} mol L^{-1} in acetonitrile, in the range 200–600 nm. The weak bands centered at 331 nm for **I** and 345 nm for **II** are attributed to intramolecular charge transfer transitions from the p_{π} orbital on the

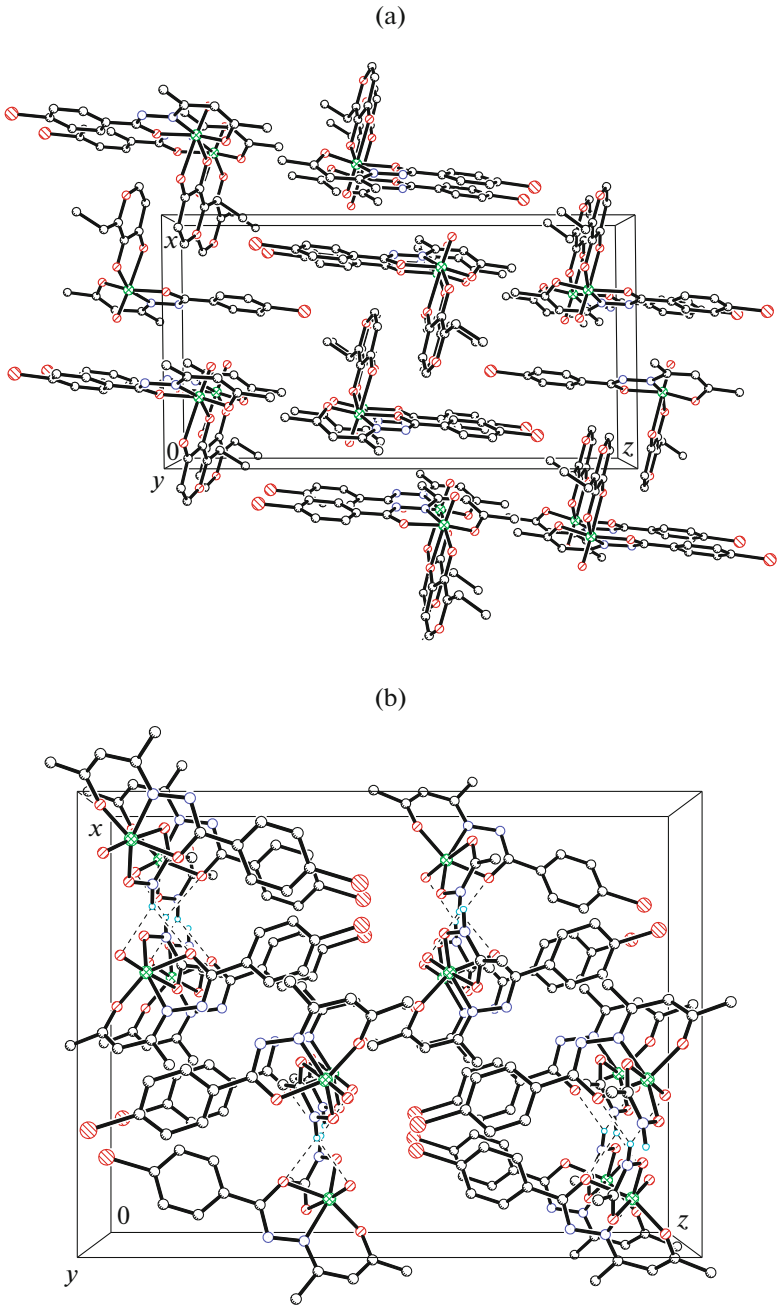

Fig. 2. Crystal packing of **I** (a) and **II** (b), viewed along the *y* axis. Hydrogen bonds are shown as dashed lines.

nitrogen and oxygen to the empty *d* orbitals of the metal [21]. The intense bands observed at 275 nm for the complexes are assigned to intraligand π–π* transition [21].

The complexes were screened for antibacterial activities against two Gram-positive bacterial strains (*B. subtilis* and *S. aureus*) and two Gram-negative bacterial strains (*E. coli* and *P. aeruginosa*) by MTT method. The IC_{50} values of the complexes against the bacteria are presented in Table 3. Penicillin G was tested as a reference drug. Complex **I** and **II** exhibited

Table 3. Antibacterial results (IC_{50}, μg mL^{-1})

Compound	Gram-positive		Gram-negative	
	B. subtilis	*S. aureus*	*E. coli*	*P. aeruginosa*
I	2.81	>50	>50	>50
II	18.96	>50	>50	>50
Penicillin G	2.35	0.75	17.51	17.49

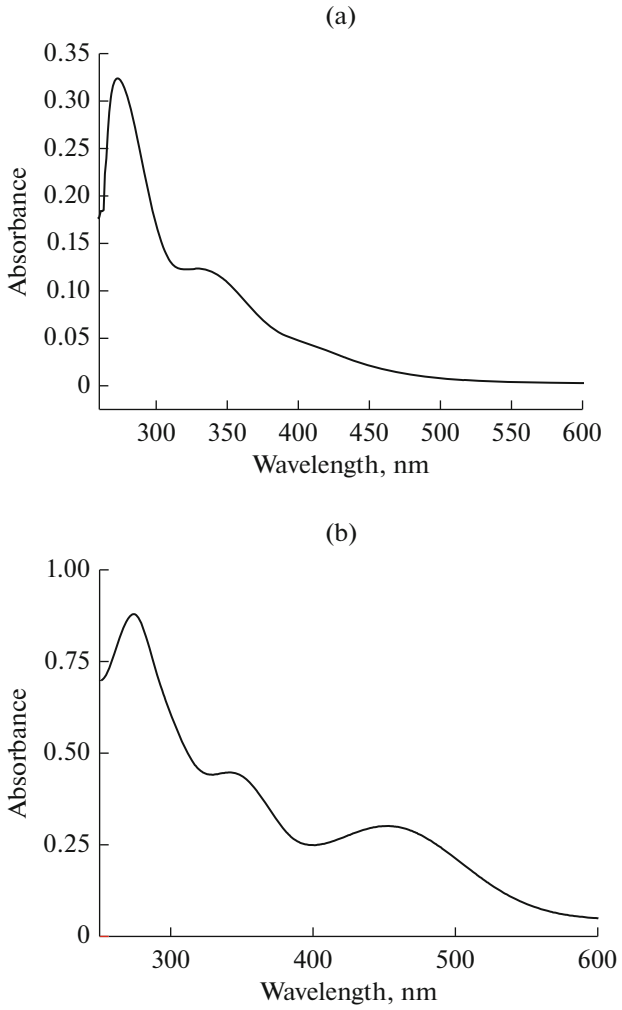

Fig. 3. UV-Vis spectrums of **I** (a) and **II** (b).

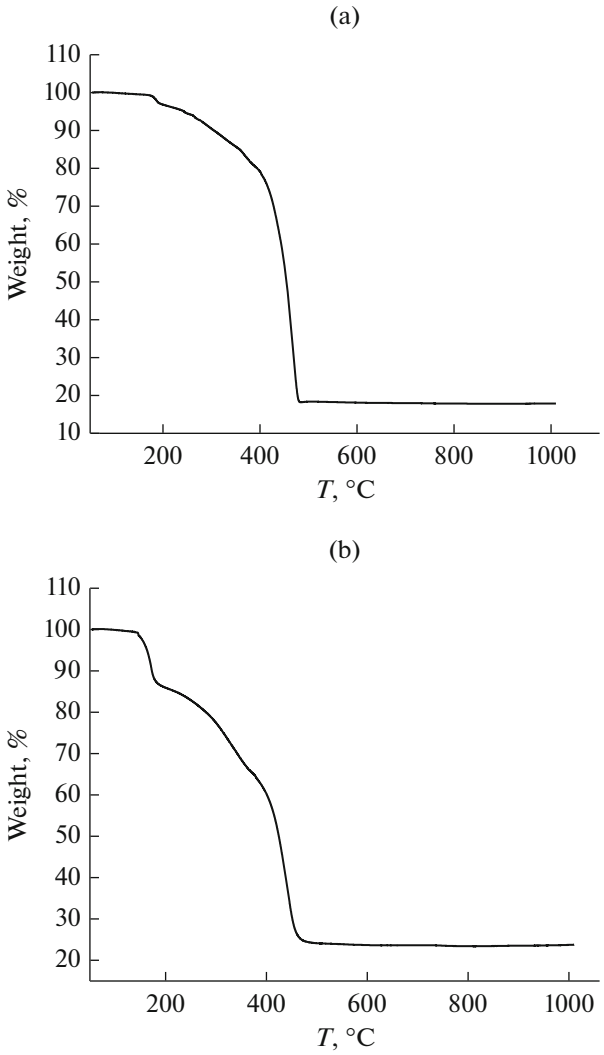

Fig. 4. TG curves of complexes **I** (a) and **II** (b).

effective activities against *B. subtilis*, while no activity against *S. aureus*, *E. coli* and *P. aeruginosa*. Obviously, complex **I** is more effective against *B. subtilis* than complex **II**. Interestingly, the IC_{50} value of complex **I** (2.81 μg mL^{-1}) is similar to that of Penicillin G (2.35 μg mL^{-1}).

TG analysis was conducted from 50 to 1000°C under air atmosphere at a heating rate of 10°C/min to examine the stability of the complexes (Fig. 4). The decomposition of **I** started at 170°C and completed at 485°C. The observed weight loss of 81.9% is close to the calculated value (81.8%) with the final product of V_2O_5. The decomposition of **II** started at 140°C and completed at 485°C. The observed weight loss of 78.5% is close to the calculated value (79.1%) with the final product of V_2O_5.

ACKNOWLEDGMENTS

This work was financially supported by K.C. Wong Magna Fund in Ningbo University, and the Open Laboratory Program of Liaoning Normal University (project no. cx20160102).

REFERENCES

1. Chans, G.M., Nieto-Camacho, A., Ramirez-Apan, T., et al., *Aust. J. Chem.*, 2016, vol. 69, no. 3, p. 279.
2. Qureshi, F., Khuhawar, M.Y., Jahangir, T.M., et al., *Acta Chim. Slov.*, 2016, vol. 63, no. 1, p. 113.
3. Adhikary, J., Kundu, P., Dasgupta, S., et al., *Polyhedron*, 2015, vol. 101, p. 93.
4. El-Gammal, O.A., *Inorg. Chim. Acta*, 2015, vol. 435, p. 73.
5. Mba, M., Pontini, M., Lovat, S., et al., *Inorg. Chem.*, 2008, vol. 47, no. 19, p. 8616.
6. Zhang, X.A. and Woggon, W.D., *J. Am. Chem. Soc.*, 2005, vol. 127, no. 41, p. 14138.
7. Zhang, X.A., Meuwly, M., and Woggon, W.D., *J. Inorg. Biochem.*, 2004, vol. 98, no. 11, p. 1967.

8. Farzanfar, J., Ghasemi, K., Rezvani, A.R., et al., *J. Inorg. Biochem.*, 2015, vol. 147, p. 54.
9. Pawar, V., Joshi, S., and Uma, V., *Asian J. Chem.*, 2013, vol. 25, no. 3, p. 1497.
10. Sheikhshoaie, I., Ebrahimipour, S.Y., Lotfi, N., et al., *Inorg. Chim. Acta*, 2016, vol. 442, p. 151.
11. He, M., Jiao, Q.Z., Chen, X.F., et al., *Chin. J. Inorg. Chem.*, 2015, vol. 31, no. 8, p. 1590.
12. Ren, J.Q., Jiao, Q.Z., Wang, Y.N., et al., *Chin. J. Inorg. Chem.*, 2014, vol. 30, no. 3, p. 640.
13. Zhao, X.L., Chen, X.F., Li, J., et al., *Polyhedron*, 2015, vol. 97, p. 268.
14. *SMART (version 5. 624) and SAINT (version 6.04*), *Programs Using the Windows NT System*, Madison: Bruker AXS Inc., 2001.
15. Sheldrick, G.M., *SADABS, Program for Empirical Absorption Correction of Area Detector*, Göttingen: Univ. of Göttingen, 1996.
16. Sheldrick, G.M., *Acta Crystallogr., Sect. A: Found. Crystallogr.*, 2008, vol. 64, no. 1, p. 112.
17. Patra, D., Biswas, N., Mondal, B., et al., *Polyhedron*, 2012, vol. 48, no. 1, p. 264.
18. Jin, Y.S. and Lah, M.S., *Eur. J. Inorg. Chem.*, 2005, no. 24, p. 4944.
19. You, Z.-L., Xian, D.-M., and Zhang, M., *CrystEngComm*, 2012, vol. 14, no. 21, p. 7133.
20. Sangeetha, N.R., Kavita, V., Wocadlo, S., et al., *J. Coord. Chem.*, 2000, vol. 51, no. 1, p. 55.
21. Asgedom, G., Sreedhara, A., Kivikoski, J., et al., *J. Chem. Soc., Dalton Trans.*, 1996, no. 1, p. 93.